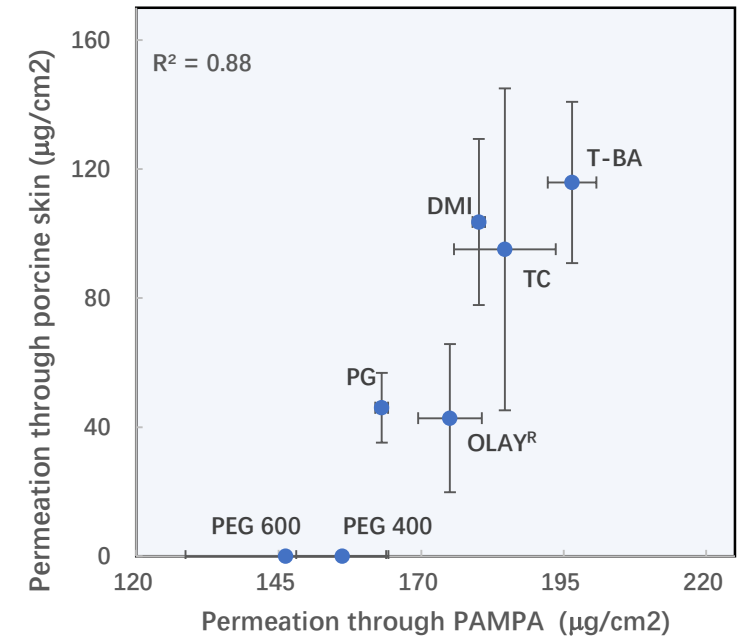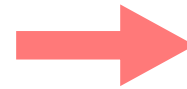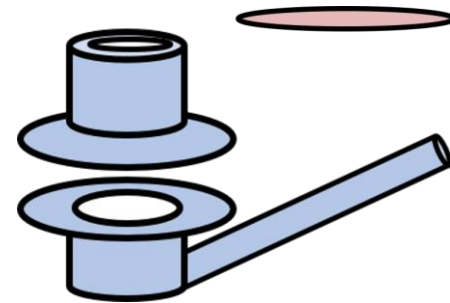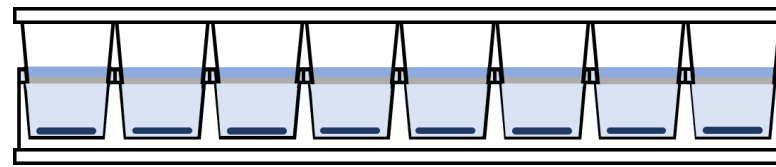A comparison of the *in vitro* permeation of niacinamide in mammalian skin and in the Parallel Artificial Membrane Permeation Assay (PAMPA) model

Yanling Zhang [a]*, Majella E. Lane [a], Jonathan Hadgraft [a], Michael Heinrich[a], Tao Chen[b], Guoping Lian[b,c] ,Balint Sinko [d]

[a] UCL School of Pharmacy, 29–39 Brunswick Square, WC1N 1AX London, UK

[b] University of Surrey, Guildford, GU27XH, UK

[c] Unilever Research Colworth, Colworth Park, Sharnbrook, Bedfordshire, MK401LQ, UK.

[d] Pion Inc., 10 Cook Street, Billerica, MA 01821, United States

*Corresponding author.

E-mail address: yanling.zhang.15@ucl.ac.uk (Y. ZHANG),

Telephonehone number: 07421316748

Abstract

The *in vitro* skin penetration of pharmaceutical or cosmetic ingredients is usually assessed in human or animal tissue. However, there are ethical and practical difficulties associated with sourcing these materials; variability between donors may also be problematic when interpreting experimental data. Hence, there has been much interest in identifying a robust and high throughput model to study skin permeation that would generate more reproducible results. Here we investigate the permeability of a model active, niacinamide (NIA), in (i) conventional vertical Franz diffusion cells with excised human skin or porcine skin and (ii) a recently developed Parallel Artificial Membrane Permeation Assay (PAMPA) model. Both finite and infinite dose conditions were evaluated in both models using a series of simple NIA solutions and one commercial preparation. The Franz diffusion cell studies were run over 24 h while PAMPA experiments were conducted for 2.5 h. A linear correlation between both models was observed for the cumulative amount of NIA permeated in tested models under finite dose conditions. The corresponding correlation coefficients (r^2) were 0.88 for porcine skin and 0.71 for human skin. These results confirm the potential of the PAMPA model as a useful screening tool for topical formulations. Future studies will build on these findings and expand further the range of actives investigated.

1. Introduction

A wide range of actives target the skin for therapeutic or cosmetic purposes. The stratum corneum (SC) is the outermost layer of the skin and it has been identified as the major barrier to the penetration of drugs and xenobiotics (Hadgraft and Lane, 2005). Structurally the human SC comprises layers of dead, keratinized cells with an intercellular matrix comprised of largely ceramides, cholesterol and free fatty acids (Wertz, 2005). Theoretically, molecules may penetrate the skin through the SC lipids (intercellular route), by sequential partitioning from the corneocytes and the lipids (transcellular route) or by accessing skin appendages (hair follicles, sweat glands). However, our current understanding indicates that for most compounds, it is diffusion through the skin lipids that is important for effective skin penetration (Hadgraft and Lane, 2016).

Excised human skin is the "gold-standard" tissue to evaluate the feasibility of transdermal and topical delivery of chemicals (Franz, 1975). However, human tissue is often difficult to source, expensive and ethical concerns are raised widely. Porcine skin has been recognized as an appropriate tissue for prediction of human skin permeability for some years, despite the lower barrier function of this tissue compared with human skin (Schmook et al., 2001; Vallet et al., 2007; Barbero and Frasch, 2009; Luo et al., 2016; Yoshimatsu et al., 2017).

A number of human skin equivalents (HSEs) have also been developed and investigated to determine their suitability as human skin permeation models (Ponec et al., 2001; Netzlaff et al., 2005; Mathes et al., 2014). HSEs are typically constructed by culturing human keratinocytes on appropriate substrates (Mathes et al., 2014). Although some HSEs have been validated for assessment of skin irritation (Fentem and Botham, 2002; Alépée et al., 2010), they have not proved useful for prediction of skin permeability because of their comparatively low barrier function (Mathes et al., 2014).

The Parallel Artificial Membrane Permeation Assay (PAMPA) model was originally developed by Kansy and coworkers as a high-throughput screening tool to study passive membrane permeability of drugs (Kansy et al., 1998). It has subsequently been used to study gastrointestinal absorption (Bujard et al., 2014) and drug permeability across the blood-brain barrier (Di et al., 2009). The PAMPA technique was first investigated for prediction of skin permeability by Ottaviani et al. (2006). In this study, the membranes used to mimic the human skin barrier were filters, which are immobilized with either isopropyl myristate or silicone oil, or mixtures of the two components. Subsequently the "Skin PAMPA" was refined by Sinkó et al. (2012) and currently state-of-the-art is a 96-well plate asay with a lipid membrane. The membrane itself is composed of free fatty acids, cholesterol and a synthetic ceramide analogue (certamide). Recently, Luo et al. (2016) investigated the permeation of the lipophilic molecule ibuprofen (LogP ($_{octanol/water}$) = 4.0, (Moffat et al., 2010) using an artificial membrane (silicone), porcine tissue, human skin and the PAMPA model. Under finite dose conditions, the most efficient formulation, as assessed using human skin, also delivered the highest amount of ibuprofen in the

PAMPA model. Clear differences in drug delivery from different formulation types (solution vs. gel) were also evident in the PAMPA model but not in the other models. The PAMPA model has also recently been used to evaluate formulations for transdermal delivery (Vizserálek et al., 2015; Balazs et al., 2016). However, to our knowledge no other studies have examined or attempted to validate PAMPA as a tool for predicting topical drug delivery outcomes.

Niacinamide (NIA), is the amide form of vitamin B3 and is a hydrophilic compound with a low molecular weight (Table 1). It is used in cosmetic and personal care formulations for the management of a number of dermatological conditions, including melanogenesis, acne, atopic dermatitis, aging of the skin and ultraviolet-induced DNA damage (Lee et al., 2016; Papich, 2016). Mohammed et al. (2013) also demonstrated that repeated application of NIA formulations to the forearms of human subjects increased SC barrier function. Therefore, the objectives of the present work were

(i) to investigate the suitability of the Skin PAMPA model for prediction of NIA skin permeation and

(ii) to identify optimal dosing and experimental conditions for NIA formulations in the PAMPA model.

The vehicles selected for NIA formulations were propylene glycol (PG), PEG 400, PEG 600, dimethyl isosorbide (DMI), t-Butyl alcohol (T-BA), and Transcutol® (TC); these solvents were chosen because of their GRAS status and widespread use in skin preparations.

2. Materials and methods

2.1 Materials

NIA was obtained from Sigma Aldrich, UK. HPLC grade water, methanol, PG, PEG 400 and PEG 600 were purchased from Fisher Scientific, UK. DMI and T-BA were kindly donated by Croda Ltd. (Goole, UK). TC was donated by Gattefossé, St. Priest, France. Phosphate buffered saline (PBS) tablets were purchased from Oxoid, UK. Porcine tissue was obtained from a local abattoir. Excised abdominal human tissue was obtained from the UK Human Tissue Bank with appropriate institutional and ethical approval. The Skin PAMPA model, hydration solution, stirring disks and Gut-Box™ were supplied by pION Inc. Billerica, USA. The commercial control NIA product was OLAY® Total Effects 7 (Procter & Gamble, UK) and was purchased from a local pharmacy.

2.2 Solubility, solubility parameter and stability determination and preparation of NIA formulations

The Hildebrand and van Krevelen solubility parameters for NIA and vehicles were calculated using Molecular Modelling Pro® (Version 6.3.3, ChemSW, Fairfield, CA, USA). The stability of

NIA in selected solvents was examined over 72h at 32 ± 1 ℃. The studies were conducted by preparing solutions of known concentrations of NIA in the solvents (n=3). The solution was placed in glass tubes with screw caps and the tubes were sealed with Parafilm® and placed in a water bath at 32 ± 1 ℃. Samples were withdrawn at 0, 24, 48 and 72h. All samples were subsequently analyzed by HPLC (Section 2.3). Solutions of NIA (5% w/v) were prepared in PG, PEG 400, PEG 600, DMI, T-BA and TC.

2.3 HPLC analysis and method validation

NIA analysis was conducted using a HPLC equipped with an Agilent G1322A degasser, G1311A quaternary pump, G1313A auto sampler, G1316A thermostat column compartment and G1315B detector. ChemStation® Rev. A.09.03 (Agilent Technologies, U.S.A.) software was used to analyse the data. NIA was analyzed with a Kinetix® 5 μm Phenyl-Hexyl 250 x 4.6 mm reversed phase column (Phenomenex, U.K.) packed with a SecurityGuard™ Phenyl-Hexyl cartridge (Phenomenex, U.K.). The mobile phase consisted of water:methanol (80:20). The injection volume was set to 10 μL. The UV detector was set to 263 nm, and the flow rate was 1 mL/min with the column temperature at 30 ℃. Linearity, accuracy, precision, detection limit (LOD), quantitation limit (LOQ) and robustness of this method were validated according to ICH guidelines (2005). HPLC analysis calibration curves (ranging from 0.5 to 100 μg/ml) were constructed. The linearity was confirmed by the r^2 value of 0.99. The retention time of NIA was 3.62 min. Accuracy was evaluated by investigating NIA recoveries at three different concentrations. A recovery within the range of 94 to 100.35% was achieved. Precision was assessed by determination of inter-day variability and intra-day repeatability. The % RSD results of intra-day and inter-day precision were below 1%. The LOD and LOQ values were 0.16 and 0.49 μg/ml, respectively.

2.4 Permeation studies in human and porcine skin

Vertical glass Franz diffusion cells were used to perform the studies in human skin and full thickness porcine ear skin as reported previously (Oliveira et al., 2012). Both finite and pseudo-finite doses (5 and 50 μl/cm²) of the NIA solutions and commercial formulation were used for all skin experiments. The human skin was prepared by heat separation (Kligman and Christophers, 1963), and porcine ear skin was prepared as described in detail by Caon et al. (2010). Heat separation of porcine skin was not carried out as it has been shown to compromise the tissue integrity. Skin samples were stored in the freezer at -20 °C until required. Before use, skin integrity was examined by assessment of electrical resistance (Oliveira et al., 2012). Degassed freshly prepared PBS solution (pH 7.30 ± 0.10) was used as the receptor medium. The permeation study was conducted for 24 h at 32 ± 1 ° C. The drug solutions were applied once the temperature of the skin surface had equilibrated to 32 ± 1 ° C (TM-22 Digitron digital thermometer, RS Components, Corby, UK). At each sampling interval up to 24 h, a volume of

200 µl of receptor medium was withdrawn and an equal volume of PBS solution was added. All samples were analysed by HPLC. After the permeation study, the receptor medium was removed completely. The mass balance study was conducted and validated. The skin surface was washed three times with 1 ml of methanol-water (50:50) mixture for finite dose studies and five times for infinite dose studies. The skin was removed from the Franz cell and placed in an Eppendorf® tube with 1 ml of methanol-water (50:50). All the tubes were placed in a rotor (rotating at 40 rpm) in a temperature-controlled oven ($32\pm0.5^{\circ}$ C) overnight. After extraction was completed, the tube was centrifuged at 13,000 rpm at 32° C for 15 min. Aliquots were taken from the supernatant portion and analysed by HPLC in order to quantify the amounts of NIA on the surface of the skin and inside the skin.

2.5 Skin PAMPA permeation studies

The Skin PAMPA model was prepared as described previously, and permeation studies were conducted using a modified protocol and the doses selected here are the same as those investigated by Luo et al. (2016), Two different doses of the NIA solutions and the commercial formulation were investigated, 1 and 30 µl per donor well, corresponding to 3 and 90 µl/cm² of preparations, respectively. These doses were selected based on previous experience with dosing of ibuprofen in PAMPA (Luo et al., 2016). Figure 1 shows the schematic of the Skin PAMPA system. The 96-well plate on the top side was selected as the donor plate and the formulation was applied on the membrane surface of each well on the top plate at the beginning of the experiment. The receptor medium was freshly prepared PBS solution. A volume of 180 µl was added to each well in the receptor plate. A stirring disk was placed in each well of the receptor plate. After dosing with the chosen formulations, the donor plate was placed on the receptor plate. The plates were incubated in the stirring unit of the "Gut-Box™" for 2.5 h at $32 \pm 1^{\circ}$ C as preliminary experiments had confirmed that all NIA had permeated at this time point. At 0.08, 0.17, 0.33, 0.67, 1, 1.5, 2 and 2.5 h, the receptor plate was replaced with a new 96-well plate prefilled with fresh temperature equilibrated receptor medium. 150 µl of sample solution was withdrawn from each receptor well and subsequently analyzed by HPLC.

2.6 Statistical analysis

All results are reported as the mean $\pm$ standard deviation (SD). Statistical analysis was performed using MS Excel and SPSS software (IBM SPSS Statistics, Version 24). One-way analysis of variance (ANOVA) followed by a Post Hoc Tukey test was conducted for multiple comparisons between the groups, and for groups with unequal sample sizes, the Scheffe's method was used for Post Hoc comparisons. A value of $p < 0.05$ was considered to be statistically significant. The correlation between cumulative amounts of NIA penetrated through PAMPA and skin membranes was determined using the Pearson Product-moment correlation coefficient (r^2)

with MS Excel®(Microsoft Corp., USA).

3. Results

3.1 Solubility and stability studies

Figure 2 shows the Hildebrand and Van Krevelen solubility parameters of the various solvents plotted against NIA solubility. Considering that the solubility parameter of NIA is 13.9 $(cal/cm^3)^{1/2}$ the molecule is expected to be soluble in vehicles that are also hydrophilic; the solubility of NIA ranged from 9 to 28% (w/v) in the various solvents. Clearly, NIA is more soluble in those solvents with solubility parameter values closest to that of NIA (Figure 2). Similarly, the lowest solubility value was observed in DMI, the solvent with the greatest difference in solubility parameter value to that of NIA. With the exception of TC, after 72 h stability studies at $32 \pm 1°$ C, the recovery values of NIA were > 90%; the corresponding value for TC was 88.5%. The stability of NIA in PBS solution was also confirmed (data not shown).

3.2 Porcine skin permeation and mass balance results

Two doses (5 and 50 μl cm²) of the various NIA solutions in the selected vehicles were examined for NIA *in vitro* permeation studies using porcine skin. Figures 3A and 3B show the permeation profiles for all vehicles and the commercial control over 24 h. No permeation was observed for NIA from PEG 400 and PEG 600 formulations for both finite and infinite dose conditions. After 24 h, the cumulative amounts of NIA that permeated under infinite dose conditions ranged from 38 to 474 $\mu g/cm^2$; the highest NIA permeation was observed for the T-BA solution, corresponding to ~18% of the applied dosage. However, there were no significant differences in permeation for all the formulations (p>0.05, Figure 3A). For finite dose conditions, NIA permeation ranged from 43 - 116 $\mu g/cm^2$, again with no significant differences in permeation between formulations.

The results for the mass balance studies are summarised in Table 2. For the infinite dose conditions, significantly higher amounts of the applied doses of NIA were extracted for T-BA and DMI, (20.8 and 7.6%) compared with the other vehicles (p<0.05); there were no significant differences between these two values (p>0.05). For PG, TC, PEG 400 and PEG 600 vehicles the percentages of NIA extracted from skin were 3.3, 0.8, 0.4 and 0.1%, respectively (Table 2). Results for finite dose permeation studies conditions indicate no skin retention of NIA for PEG 400 and corresponding values for PEG 600, PG, TC, DMI, T-BA and the commercial formulation were 0.7, 2.7, 16.4, 16.7, 4.9 and 24.5%, respectively. NIA was delivered into the skin for the higher molecular weight PEG but not the lower molecular weight vehicle; this may reflect the significantly higher solubility of NIA in the lower molecular weight PEG (Figure 2). The skin extraction of NIA from the commercial product was significantly higher than from PG, T-BA and PEG 600 (p<0.05).

3.3 Human skin permeation and mass balance studies

As for the results observed for porcine tissue, no permeation of NIA was observed for PEG 400 and PEG 600 for both finite and infinite dose conditions (Table 3). For the infinite dose studies with the other vehicles, the cumulative amounts of NIA that permeated through human skin ranged from 1.5 – 169.2 µg/cm². A significantly higher amount of NIA permeated from T-BA compared with all other formulations (p<0.05). Under finite dose conditions, the highest permeation of NIA was observed for T-BA (50.8 µg/cm², p<0.05) and the cumulative amounts of NIA that permeated from TC, DMI, PG and the commercial formulation were 16.4 ± 4.6, 15.0 ± 3.4, 1.8 ± 0.4 and 5.3 ± 1.5 µg/cm², respectively. No significant differences in permeation were found between TC, DMI, PG and the commercial formulation (p>0.05).

Results from the mass balance studies confirmed that more than 80% of the applied amounts of NIA remained on the skin surface for all vehicles under infinite dose conditions. The corresponding amounts of NIA retained in the skin were also less than 2% for all vehicles under infinite dose conditions, and a significantly higher amount of NIA was extracted for PG than for other formulations (p<0.05, Table.2.). Comparatively higher percentages of NIA were extracted for all vehicles for finite dose studies compared with infinite dose studies (p<0.05), with values ranging from 1.51% for PEG 400 to 32.89% for TC. Excluding T-BA and DMI, the percentage of NIA extracted for TC was also significantly higher than the remaining formulations (p<0.05).

Under finite dose conditions, the permeation through human skin was significantly lower than permeation through porcine skin (p<0.05). The higher percutaneous delivery of NIA in porcine skin compared with human skin is also similar to the results observed by other researchers (Dick and Scott, 1992; Singh et al., 2002; Barbero and Frasch, 2009; Luo et al., 2016).

3.4 Skin PAMPA permeation studies

Two doses of the various formulations of NIA in the selected vehicles were investigated in the Skin PAMPA membrane, namely 1 and 30 µl per well, corresponding to 3 and 90µl/cm² concentrations based on our previous publication (Luo et al., 2016). The permeation profiles of NIA in the Skin PAMPA model are shown in Figure 4. For the 30 µl applications, a significantly higher cumulative amount of NIA permeation was evident for the T-BA formulation compared with all other formulations (p<0.05). Under finite dose conditions, the rank order for cumulative amounts of NIA that permeated was the same as for finite doses in human skin at 24 h. However, no significant differences between formulations were evident (p>0.05). Although no permeation was observed in porcine or human skin for PEG 400 and PEG 600, in the PAMPA model NIA permeation was observed for both vehicles for both infinite and finite doses.

Under infinite dose conditions, for PEG 400 and PEG 600 significantly lower cumulative amounts of NIA permeated (397.7 and 425.7 µg/cm², respectively) compared to all other formulations (p<0.05). The corresponding values of NIA permeation for PEG 400 and PEG 600 for the 1 ul application were 146.3 and 156.2 µg/cm²; however, at the lower doses these values

were not statistically different from other formulations ($p > 0.05$). Curvilinear permeation profiles of NIA following the 1 µl application were evident for all formulations (Figure 4), presumably reflecting donor depletion. The permeation profiles were generally linear for the 30 µl dose also consistent with this corresponding to an infinite dose of the formulation. Values for percentage permeation of NIA in PAMPA are shown in Table 4. For the 1 µl dose, all formulations delivered more than 90 % of the applied amounts of NIA in PAMPA at 2.5 h; in porcine skin and human skin values ranged from 1 – 24 and 18 – 55 %, respectively. For the 30 µl dose, lower values were observed ranging from 7% to 52 % at 2.5 h (Table 4). Higher permeation of NIA is evident in the Skin PAMPA model for both finite and infinite doses ($p < 0.05$). This is in line with the results from the previous investigation of ibuprofen permeation in human and porcine skin and PAMPA by Luo et al. (2016). The NIA permeation in the various models may be ranked as follows: Skin PAMPA model > Porcine skin > Human skin.

The permeation data for finite dose skin permeation experiments for PAMPA are plotted against corresponding values for the porcine and human skin studies in Figure 5. A correlation coefficient (R^2) of 0.88 was observed for the linear regression of porcine skin (Figure 5A) and PAMPA data, with a value of 0.71 obtained for human skin and PAMPA results (Figure 5B). Although attempts were made to fit the data to an exponential model and to determine similar r^2 values for infinite dose conditions, no correlations were observed. Considering the variability in porcine and human skin the correlations observed here are encouraging and warrant further development of PAMPA as a screening tool for human skin permeability.

A robust, high-throughput skin surrogate has been of considerable interest to the personal care and pharmaceutical industries for many years. The tissue architecture and quality of the permeability barrier in commercially available reconstructed human skin models; EpiDerm, SkinEthic and Episkin in comparison to native tissue was examined by Ponec et al. (2000). In these three skin models the epidermis was reconstructed by culturing normal human keratinocytes at the air-liquid interface. Although the authors noted that the three skin models provided a promising means for studying the effects of topically applied chemicals, the barrier properties of the tissues were not optimal. In a later study the same group investigated a stratum corneum substitute (SCS) composed of cholesterol, ceramides and free fatty acids mounted on a polycarbonate support (de Jager et al., 2006). The model permeants p-aminobenzoic acid (PABA), ethyl PABA and butyl PABA were investigated; for all three model compounds, the authors reported that the permeability characteristics of the SCS with a 12-µm-thick lipid layer closely resembled those of human SC. However, comparisons of this work with the present study are not possible because only infinite doses were examined and dermatomed skin was used.

The influence of lipid composition, and specifically the physicochemical properties of ceramides on model membrane permeability has been extensively investigated by Vávrová and co-workers (Vávrová et al., 2003; Janůšová et al., 2011; Školová et al., 2013; Paloncýová et

al., 2015; Školová et al., 2017). Janůšová et al. (2011) compared the effects of acyl chain length in the non-hydroxy acyl sphingosine type ceramides on the porcine skin permeation of two model actives, theophylline and indomethacin. The experiment was conducted using either co-application of the different ceramides with varied acyl chain length and the model drug or a pretreatment of skin with the ceramides followed by the permeation of the drugs. These authors concluded that the skin barrier properties decreased with reducing content of the short chain ceramide, and that the relationship between the ceramide acyl chain length and the skin permeability was not linear. Školová et al. (2013) assessed the permeabilities of the model SC lipid membranes with and without the native long-chain Cer24 (Cer NS, N-tetracosanoylsphingosine) again with the same permeants used in the earlier study. The presence of the long-chain ceramide was observed to be critical for measurable permeability of small hydrophilic to moderately lipophilic compounds. Enhanced permeability of a similar model containing short chain ceramides were further studied by Paloncýová et al. (2015). These workers prepared bilayers of equimolar mixtures of lignoceric acid, and cholesterol and ceramide NS (N-lignoceroylsphingosine). Water penetrated through the pure ceramide membranes and the pure ceramide bilayers were also more sensitive to acyl chain length than the other mixed systems that were evaluated. The importance of structure-permeability relationship with reference to ceramides was further highlighted in a later study by the same group (Školová et al., 2017). These researchers studied the permeability of model membranes containing ceramides with C_{24} acyl chains, specifically a phytoceramide and a dihydroceramide. The model membrane with the phytoceramide was more permeable compared with the corresponding membrane containing the dihydro)ceramide that had the same chain lengths (Školová et al., 2017).

Most recently, simplified stratum corneum models composed of stearic acid, cholesterol, cholesterol sulfate and a ceramide (CER) component consisting of N-2-hydroxystearoyl phytosphingosine (CER[AP]) and/or N-stearoyl phytosphingosine (CER[NP] were investigated by Čuříková et al. (2017) to study drug permeation and transdermal penetration enhancers. The permeation profiles of two model actives, theophylline and indomethacin were investigated in three types of CER/SA/Chol/CholS membranes, the CER part of which contained CER[AP] or CER[NP] or their 1:1 molar mixture. The mixed CER[AP]/[NP] membrane was chosen for further experiments as permeation data more closely matched results for porcine skin permeation compared with the other models. Subsequently, the effects of the transdermal penetration enhancers Azone and (S)-N-acetylproline dodecyl ester on the permeation of the model drugs was investigated. Similar trends in the permeation of the drugs were observed for both porcine skin and the model membrane but as expected enhancement ratio values were higher for the latter. As reported in the present work the time for permeation to occur in these artificial models is much shorter when compared with human or porcine tissue, consistent with the findings of Vávrová and co-workers. These simplified model membranes based on phytosphingosine CERs clearly show promise for the evaluation of permeation of hydrophilic and lipophilic compounds.

The synthetic ceramide (certamide) composition of the Skin PAMPA model investigated in the present work is proprietary (Luo et al., 2016) and cannot be disclosed at the present time. However, our data confirm that the lipid composition of the PAMPA model is clearly critical to the ability of permeants to cross this membrane.

4. Conclusions

Of all the vehicles, and for all models examined, high permeation was observed for T-BA. As there is only limited information about the ability of this tertiary alcohol to promote skin permeation, further studies will be necessary to investigate any solvent effects on skin integrity. The permeation of NIA from PEG 400 and PEG 600 vehicles in PAMPA but not in porcine or human skin suggests that the high throughput model may not be suitable for evaluating formulations containing these materials. It is also possible that the results reflect an interaction between the PAMPA membrane and the solvents; this is being investigated further.

The permeation of NIA in porcine tissue, human skin and the Skin PAMPA model confirms the lower barrier function of PAMPA compared with biological tissues. However, the correlations observed indicate that a wider range of actives should be examined to explore fully the potential of PAMPA as a high throughput model to predict skin permeation. With respect to human and porcine skin the results confirm the lower permeability of the latter compared with the former consistent with the work of other researchers. Additionally, the importance of conducting finite versus infinite dose skin permeation studies is underlined once more; finite dose conditions better simulate the application of topical formulations to the skin in the real world. Ultimately, the development and validation of a reliable, robust and reproducible human skin surrogate should deliver considerable benefits for government, the personal care sector, the pharmaceutical industry, patients and consumers.

5. References

Alépée, N., Tornier, C., Robert, C., Amsellem, C., Roux, M.-H., Doucet, O., Pachot, J., Méloni, M., de Brugerolle de Fraissinette, A., 2010. A catch-up validation study on reconstructed human epidermis (SkinEthic™ RHE) for full replacement of the Draize skin irritation test. Toxicol. In Vitro 24, 257-266.

Balazs, B., Vizserálek, G., Berkó, S., Budai-Szűcs, M., Kelemen, A., Sinkó, B., Takács-Novák, K., Szabó-Révész, P., Csányi, E., 2016. Investigation of the Efficacy of Transdermal

Penetration Enhancers Through the Use of Human Skin and a Skin Mimic Artificial Membrane. J. Pharm. Sci. 105, 1134-1140.

Barbero, A.M., Frasch, H.F., 2009. Pig and guinea pig skin as surrogates for human in vitro penetration studies: A quantitative review. Toxicol. In Vitro 23, 1-13.

Bujard, A., Sol, M., Carrupt, P.-A., Martel, S., 2014. Predicting both passive intestinal absorption and the dissociation constant toward albumin using the PAMPA technique. Eur. J. Pharm. Sci. 63, 36-44.

Caon, T., Costa, A.C., de Oliveira, M.A., Micke, G.A., Simões, C.M., 2010. Evaluation of the transdermal permeation of different paraben combinations through a pig ear skin model. Int. J. Pharm. 391, 1-6.

Čuříková, B.A., Procházková, K., Filková, B., Diblíková, P., Svoboda, J., Kováčik, A., Vávrová, K., Zbytovská, J., 2017. Simplified stratum corneum model membranes for studying the effects of permeation enhancers. Int. J. Pharm. 534, 287-296.

de Jager, M., Groenink, W., Bielsa i Guivernau, R., Andersson, E., Angelova, N., Ponec, M., Bouwstra, J., 2006. A Novel in Vitro Percutaneous Penetration Model: Evaluation of Barrier Properties with P-Aminobenzoic Acid and Two of Its Derivatives. Pharm. Res. 23, 951-960.

Di, L., Kerns, E.H., Bezar, I.F., Petusky, S.L., Huang, Y., 2009. Comparison of blood–brain barrier permeability assays: in situ brain perfusion, MDR1-MDCKII and PAMPA-BBB. J. Pharm. Sci. 98, 1980-1991.

Dick, I.P., Scott, R.C., 1992. Pig ear skin as an in-vitro model for human skin permeability. J. Pharm. Pharmacol. 44, 640-645.

Fentem, J.H., Botham, P.A., 2002. ECVAM's activities in validating alternative tests for skin

corrosion and irritation. Altern. Lab. Anim. 30, 61-68.

Franz, T.J., 1975. Percutaneous absorption. On the relevance of in vitro data. J. Invest. Dermatol. 64, 190-195.

Hadgraft, J., Lane, M.E., 2005. Skin permeation: The years of enlightenment. Int. J. Pharm. 305, 2-12.

Hadgraft, J., Lane, M.E., 2016. Advanced topical formulations (ATF). Int. J. Pharm. 514, 52-57.

Janůšová, B., Zbytovská, J., Lorenc, P., Vavrysová, H., Palát, K., Hrabálek, A., Vávrová, K., 2011. Effect of ceramide acyl chain length on skin permeability and thermotropic phase behavior of model stratum corneum lipid membranes. Biochim. Biophys. Acta. 1811, 129-137.

Kansy, M., Senner, F., Gubernator, K., 1998. Physicochemical high throughput screening: parallel artificial membrane permeation assay in the description of passive absorption processes. J. Med. Chem. 41, 1007-1010.

Kligman, A.M., Christophers, E., 1963. Preparation of isolated sheets of human stratum corneum. Arch. Dermatol. 88, 702-705.

Lee, M.-H., Lee, K.-K., Park, M.-H., Hyun, S.-S., Kahn, S.-Y., Joo, K.-S., Kang, H.-C., Kwon, W.-T., 2016. In vivo anti-melanogenesis activity and in vitro skin permeability of niacinamide-loaded flexible liposomes (Bounsphere™). J. Drug Deliv. Sci. Technol. 31, 147-152.

Luo, L., Patel, A., Sinko, B., Bell, M., Wibawa, J., Hadgraft, J., Lane, M.E., 2016. A comparative study of the in vitro permeation of ibuprofen in mammalian skin, the PAMPA model and silicone membrane. Int. J. Pharm. 505, 14-19.

Mathes, S.H., Ruffner, H., Graf-Hausner, U., 2014. The use of skin models in drug development. Adv Drug Deliv Rev 69-70, 81-102.

Moffat, A.C., Osselton, M.D., Widdop, B., 2010. Clarke's Analysis of Drugs and Poisons. Sage Publications, London.

Mohammed, D., Crowther, J.M., Matts, P.J., Hadgraft, J., Lane, M.E., 2013. Influence of niacinamide containing formulations on the molecular and biophysical properties of the stratum corneum. Int. J. Pharm. 441, 192-201.

Netzlaff, F., Lehr, C.M., Wertz, P.W., Schaefer, U.F., 2005. The human epidermis models EpiSkin®, SkinEthic® and EpiDerm®: An evaluation of morphology and their suitability for testing phototoxicity, irritancy, corrosivity, and substance transport. Eur. J. Pharm. Biopharm. 60, 167-178.

Oliveira, G., Hadgraft, J., Lane, M.E., 2012. The influence of volatile solvents on transport across model membranes and human skin. Int. J. Pharm. 435, 38-49.

Ottaviani, G., Martel, S., Carrupt, P.-A., 2006. Parallel Artificial Membrane Permeability Assay: A New Membrane for the Fast Prediction of Passive Human Skin Permeability. J. Med. Chem. 49, 3948-3954.

Paloncýová, M., Vávrová, K., Sovová, Ž., DeVane, R., Otyepka, M., Berka, K., 2015. Structural Changes in Ceramide Bilayers Rationalize Increased Permeation through Stratum Corneum Models with Shorter Acyl Tails. J. Phys. Chem. B. 119, 9811-9819.

Papich, M.G., 2016. Niacinamide, Saunders Handbook of Veterinary Drugs (Fourth Edition). W.B. Saunders, St. Louis, pp. 562-563.

Ponec, M., Boelsma, E., Weerheim, A., Mulder, A., Bouwstra, J., Mommaas, M., 2000. Lipid

and ultrastructural characterization of reconstructed skin models. Int. J. Pharm. 203, 211-225.

Ponec, M., Gibbs, S., Pilgram, G., Boelsma, E., Koerten, H., Bouwstra, J., Mommaas, M., 2001. Barrier function in reconstructed epidermis and its resemblance to native human skin. Skin Pharmacol. Physiol. 14, 63-71.

Schmook, F.P., Meingassner, J.G., Billich, A., 2001. Comparison of human skin or epidermis models with human and animal skin in in-vitro percutaneous absorption. Int. J. Pharm. 215, 51-56.

Singh, S., Zhao, K., Singh, J., 2002. In vitro permeability and binding of hydrocarbons in pig ear and huamn abdominal skin. Drug Chem. Toxicol. 25, 83-92.

Sinkó, B., Garrigues, T.M., Balogh, G.T., Nagy, Z.K., Tsinman, O., Avdeef, A., Takács-Novák, K., 2012. Skin–PAMPA: A new method for fast prediction of skin penetration. Eur. J. Pharm. Sci. 45, 698-707.

Školová, B., Janůšová, B., Zbytovská, J., Gooris, G., Bouwstra, J., Slepička, P., Berka, P., Roh, J., Palát, K., Hrabálek, A., Vávrová, K., 2013. Ceramides in the Skin Lipid Membranes: Length Matters. Langmuir 29, 15624-15633.

Školová, B., Kováčik, A., Tesař, O., Opálka, L., Vávrová, K., 2017. Phytosphingosine, sphingosine and dihydrosphingosine ceramides in model skin lipid membranes: permeability and biophysics. Biochim. Biophys. Acta. Biomembr. 1859, 824-834.

Vávrová, K., Hrabálek, A., Doležal, P., Šámalová, L., Palát, K., Zbytovská, J., Holas, T., Klimentová, J., 2003. Synthetic ceramide analogues as skin permeation enhancers: structure–Activity relationships. Bioorg. Med. Chem. 11, 5381-5390.

Vallet, V., Cruz, C., Josse, D., Bazire, A., Lallement, G., Boudry, I., 2007. In vitro percutaneous

penetration of organophosphorus compounds using full-thickness and split-thickness pig and human skin. Toxicol. In Vitro 21, 1182-1190.

Vizserálek, G., Berkó, S., Tóth, G., Balogh, R., Budai-Szűcs, M., Csányi, E., Sinkó, B., Takács-Novák, K., 2015. Permeability test for transdermal and local therapeutic patches using Skin PAMPA method. Eur. J. Pharm. Sci. 76, 165-172.

Wertz, P.W., 2005. Epidermal Lipids and Formation of the Barrier of the Skin, Dry Skin and Moisturizers. CRC Press, pp. 33-39.

Yoshimatsu, H., Ishii, K., Konno, Y., Satsukawa, M., Yamashita, S., 2017. Prediction of human percutaneous absorption from in vitro and in vivo animal experiments. Int. J. Pharm. 534, 348-355.
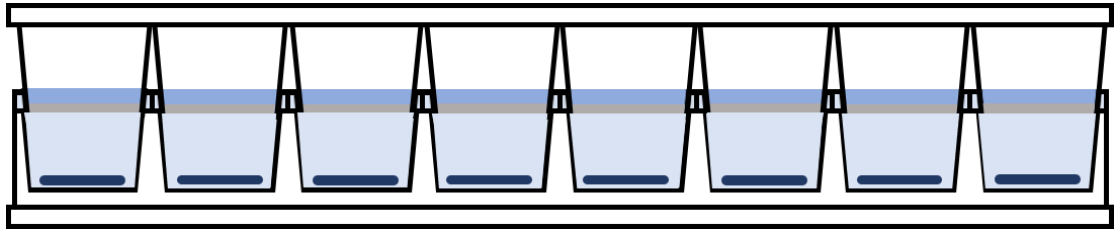
Figure(s)

Figure 1. Schematic view of the Skin PAMPA system.
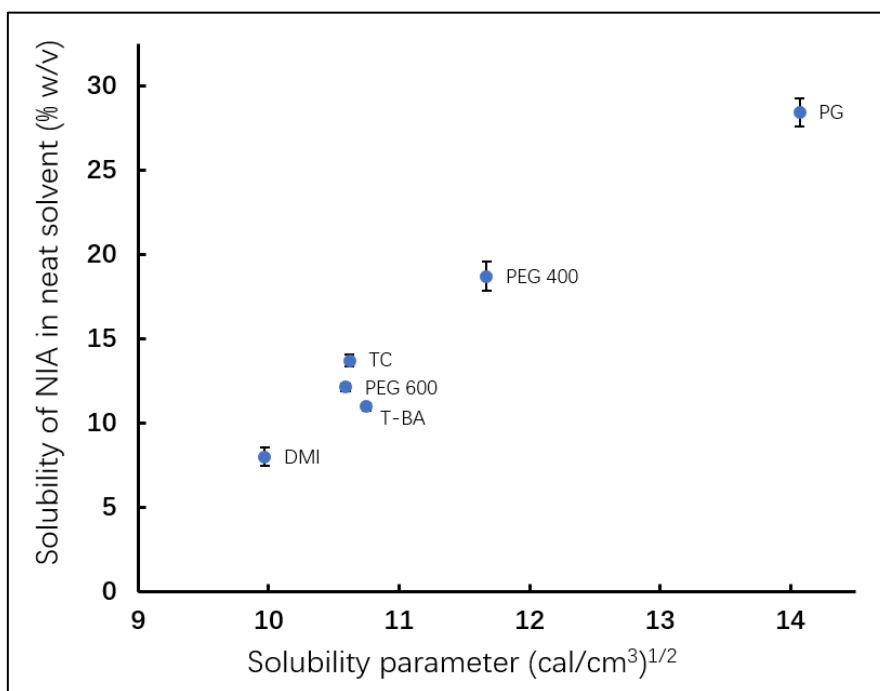
Figure 2. The Hildebrand and van Krevelen solubility parameters of solvents plotted against corresponding solubility of NIA at $32 \pm 1\,^{\circ}$C. n=3, mean $\pm$ SD.
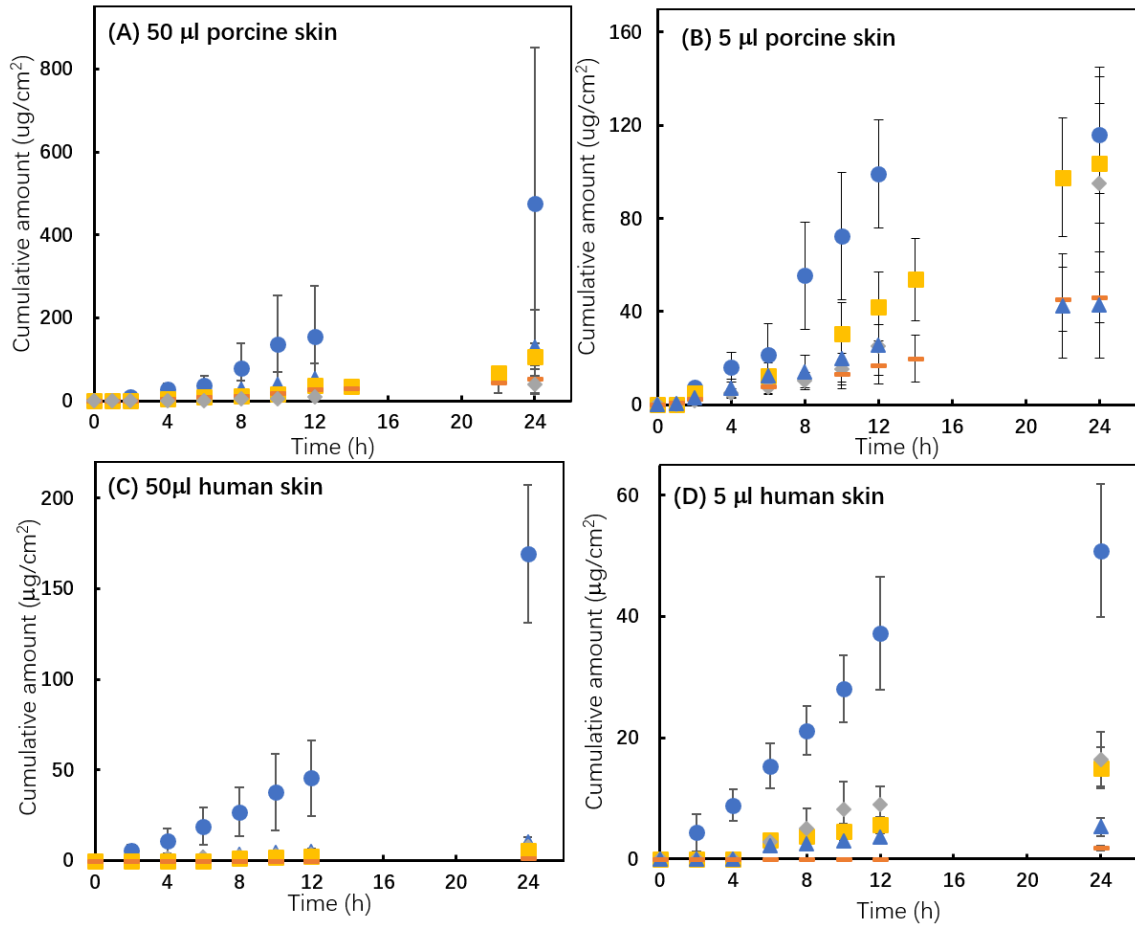
Figure 3. Cumulative amounts of NIA that permeated from OLAY®(▲), T–BA(●), PG(▬), TC(◆) and DMI (■) in porcine skin (A) and (B) and human skin (C) and (D) following application of 50 μl and 5 μl. Each data point represents the mean ± SD, 3 ≤n≤5.
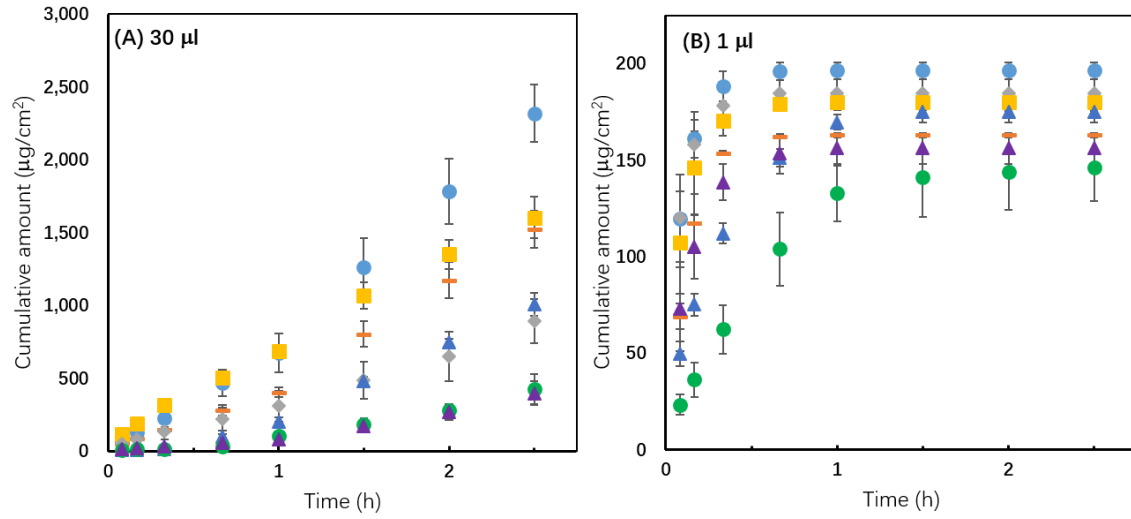
Figure 4. Cumulative amounts of NIA that permeated from OLAY®(▲), T–BA(●), PG(▬), TC(◆), DMI (■), PEG 400 (▲) and PEG 600 (●) in the Skin PAMPA model following application of 30 and 1 μl. Each data point represents the mean ± SD, n = 4.
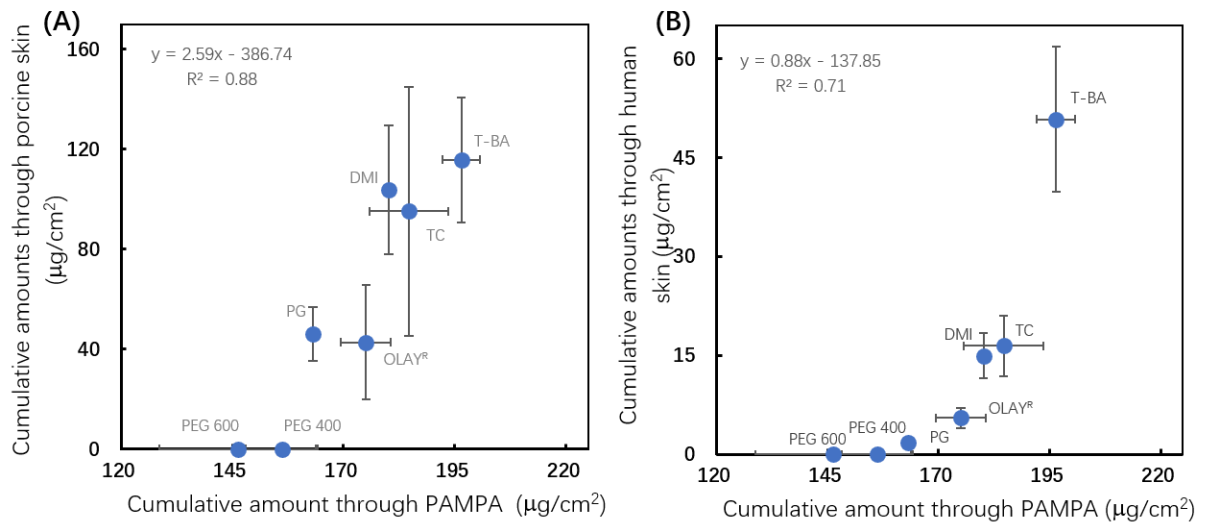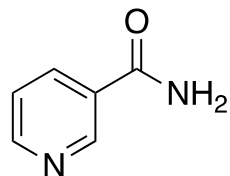
Figure 5. Correlations between the cumulative amounts of NIA that permeated through (A) porcine skin and skin PAMPA model and (B) human skin and Skin PAMPA model under finite dose conditions.

Table 1

Physicochemical properties of NIA.

Chemical structure	
Molecular weight	122.1 Da
Melting point [a]	128–131 °C
LogP ($_{octanol/water}$) [b]	−0.4
pK$_a$ [a]	3.3 (20 °C)
Solubility parameter [c]	13.9 (cal/cm^3)$^{1/2}$

[a] (O'Neil et al., 2013)

[b] (Moffat et al., 2010)

[c] Molecular Modelling Pro® (Version 6.3.3, ChemSW, Fairfield, CA, USA)

Table 2

The results of mass balance studies following the permeation studies using porcine skin under both dose conditions (3 ≤n≤5, mean ± SD)

		Formulation						
		OLAY	T–BA	PG	TC	DMI	PEG 400	PEG 600
50 μl	% Washing	75.2±11.1	45.4±21.4	96.1±8.9	81.3±0.3	90.7±3.5	87.1±12.0	87.5±11.3
	% Extraction	34.0±1.3	20.8±9.4	3.3±1.1	0.8±0.2	7.6±3.2	0.4±0.3	0.1±0.1
	% Permeation	5.1±3.0	18.0±12.7	2.3±1.4	1.5±0.7	4.4±1.4	0	0
	% Total recovery	84.2±11.8	84.1±7.0	101.7±8.2	83.6±0.4	102.7±4.7	87.5±12.1	87.6±11.4
5 μl	% Washing	42.1±12.1	20.5±2.4	55.6±7.0	33.3±15.8	8.4±2.5	89.0±17.5	100.5±1.3
	% Extraction	24.5±5.1	4.9±1.8	2.7±1.2	16.4±5.8	16.7±6.3	0	0.7±0.1
	% Permeation	18.3±11.0	54.7±11.7	19.5±5.7	38.3±18.5	48.6±13.8	0	0
	% Total recovery	84.9±10.0	80.0±7.5	77.8±3.9	88.0±10.0	73.7±11.1	89.0±17.5	101.3±1.3

Table 3

The results of mass balance studies following the permeation studies using human skin skin under both dose conditions (n=3, mean ± SD)

		Formulation						
		OLAY	T–BA	PG	TC	DMI	PEG 400	PEG 600
50 μl	% Washing	97.3±3.8	86.8±0.2	94.6±9.1	91.9±10.5	100.3±9.0	81.5±3.3	81.3±3.2
	% Extraction	0.9±0.1	0.9±0.1	1.9±0.5	0.5±0.2	0.5±0.1	0.2±0.1	0.5±0.3
	% Permeation	0.4±0.1	7.9±2.0	0.1±0.0	0.4±0.2	0.3±0.1	0	0
	% Total recovery	98.5±3.8	95.6±1.7	96.6±9.5	92.7±10.7	101.1±9.2	81.7±3.2	81.8±3.1
5 μl	% Washing	95.3±10.0	30.4±3.7	92.3±7.4	42.8±2.2	58.9±11.0	79.4±4.5	100.3±27.8
	% Extraction	5.0±0.5	25.8±4.3	12.1±8.3	32.9±11.2	18.0±0.1	1.5±0.7	1.6±0.9
	% Permeation	2.1±0.5	24.4±3.2	0.7±0.2	7.1±1.6	6.1±1.7	0	0
	% Total recovery	102.4±10.1	80.6±5.7	105.1±7.6	82.8±12.2	83.0±9.9	81.0±4.9	101.9±28.0

Table 4

Cumulative percentage permeation of NIA in the Skin PAMPA model (n = 4, mean ± SD)

	Cumulative percentage permeation at 2.5 h (%)	
	Infinite dose	Finite dose
OLAY	20.2±1.6	93.4±3.0
T–BA	52.2±4.4	99.5±2.2
PG	34.9±2.9	95.3±0.7
TC	22.3±3.7	96.8±4.7
DMI	29.2±2.6	98.4±0.6
PEG 400	9.6±2.0	95.0±4.9
PEG 600	7.5±1.9	94.6±11.4

*Conflict of Interest

<div align="center">Conflicts of interest statement</div>

I confirm that I and other authors of this manuscript have no conflict of interest to declare.

Yanling Zhang

PhD Candidate in Skin Research

UCL School of Pharmacy

London UK

Declaration of interest statement

I confirm that I and other authors of this manuscript have no conflict of interest to declare.

Yanling Zhang

PhD Candidate in Skin Research

UCL School of Pharmacy

London UK